

# PRE AND POST TEST ANALYSES OF A KKL TURBINE TRIP TEST AT 109% POWER USING RETRAN-3D

*P. Coddington*

*As part of the PSI/HSK STARS project, pre-test calculations have been performed for a KKL turbine trip test at 109% power using the RETRAN-3D code. In this paper, we first present the results of these calculations, together with a description of the test and a comparison of the results with the measured plant data, and then discuss in more detail the differences between the pre-test results and the plant measurements, including the differences in the initial and boundary conditions, and how these differences influenced the calculated results. Finally, we comment on a series of post-test and sensitivity analyses which were performed to resolve some of the discrepancies.*

*The results of the pre-test (blind) calculations show good overall agreement with the experimental data, particularly for the maximum in the steam-line mass flowrate following the opening of the turbine bypass valves. This is of critical importance, since the steam-line flow has the least margin to the reactor scram limit. The agreement is especially good since the control rod banks used for the selected rod insertion were changed from those given in the test specification.*

*Following a review of the comparison of the pre-test calculations against the measured data, several deficiencies in the RETRAN-3D model for KKL were identified and corrected as part of the post-test analysis. This allowed for both an improvement in the calculated results, and a deeper understanding of the behaviour of the turbine trip transient.*

## 1 INTRODUCTION

As part of the PSI/HSK STARS project, pre-test calculations were performed for a turbine trip test in the Kernkraftwerk Leibstadt reactor (KKL) at 109% power using the RETRAN-3D code. In this paper, we present the results of these calculations, together with a description of the test and the RETRAN-3D model of the reactor, and a comparison of the results against the measured plant data. We then discuss in some detail the differences between the pre-test calculations and the plant measurements, including the differences in the initial and boundary conditions, and how these influenced the calculated and measured results. We show through this study that it was possible to identify several deficiencies in the plant model. Finally, we comment on the post-test and sensitivity analysis which was performed to resolve some of the modelling deficiencies, and the differences in the test initial and boundary conditions. During the course of the work undertaken to perform the pre- and post-test calculations, significant modifications were made to the RETRAN-3D input model for the plant.

The pre-test analysis had two aims: first, to provide an independent set of pre-test calculations with which to examine the margin to reactor scram for a turbine trip incident at 109% power and, second, to provide an assessment of the current status of the RETRAN-3D code and the KKL model, and thereby to identify any code or model deficiencies.

## 2 TRANSIENT DESCRIPTION

A turbine trip event in KKL is characterized by the closure of the turbine stop valves (TSVs) and turbine control valves (TCVs) to protect the turbine from over-speed following loss of load on the turbine. The closure of the TCVs and TSVs produces a rapid increase in the pressure upstream of the valves as the steam

flow is temporarily reduced. Since the KKL reactor has a 110% steam bypass capacity, it is possible to divert the steam flow into the condenser by opening the bypass valves, and thereby avoid the necessity of a reactor scram for such an event. The subsequent opening of the turbine bypass valves mitigates the pressure increase, and the pressure at the turbine inlet falls. However, the opening of the bypass valves causes a surge in the steam flow along the steam line, in which the steam flowrate may rise to a value significantly above its steady-state value. The maximum in the pressure rise, and the increase in the steam mass flowrate, depend on the relative closure of the TSVs and the opening of the bypass valves; the rate at which the bypass valves open is dependant upon the bypass valve control system logic.

The increase in the pressure at the turbine inlet propagates back along the steam line as a pressure wave into the reactor pressure vessel (RPV), increasing the pressure. This then produces a collapse in the core voids, with a subsequent increase in reactor power. In order to mitigate this increase in power, and as part of the plant protection system for such events, a limited number of control rods are inserted into the core following detection of a turbine trip (or load rejection) event. The rapid insertion of these rods (referred to as SRI, or Selected Rod Insertion), reduces the power, so that no, or very little, power increase as a consequence of the void collapse is observed. In order to reduce the power over a longer time-scale, the core flow is reduced by a reduction in the re-circulation loop flow through closure of the flow control valves (FCVs).

One of the goals of the test at 109% power, and consequently one of the aims of the pre-test calculations, was to examine how close the plant protection system comes to reactor scram. There are three main measured plant scram signals which are important for this type of incident. These are the short-term re-

sponse of the main steam-line flow, the reactor pressure vessel (RPV) pressure, and the core power. The increases in the RPV pressure and main steam-line mass flowrate are strongly influenced by the closure of the TCVs and TSVs, and by the opening of the bypass valves. The short-term power response is primarily dependent upon the effectiveness of the SRI.

**3 RETRAN-3D INPUT MODEL**

For the analysis of a turbine trip, or similar transient, the RETRAN-3D input model requires three relatively independent units: a description of the plant-specific geometry, which includes the component nodalization and the initial and boundary conditions; the plant control system, which provides the steady-state control function, together with the operation of all of the plant trip and emergency protection functions which, for a turbine trip transient, dominate the calculated sequence; and the 1-D nuclear cross-sections. A RETRAN-3D BWR/6 input model had been developed previously [1,2], and used in the analysis of earlier plant start-up tests [3]. However, in order to model a turbine trip event for which the transient behaviour is dominated by the response of the plant control and protection system, a complete revision of the RETRAN-3D control system model was necessary.

The RETRAN-3D nodalization of the reactor vessel is presented in Fig. 1 and shows the lower plenum (control volumes 170 and 160), the upper plenum (150 and 140), with the core region lying between these two regions, the steam/water separator (130 and 120), the steam dome (110 and 100), and downcomer region (500 to 570). The feedwater enters the vessel at control volume 530 and the steam flows out into the steam line from control volume 500. The steam-line nodalization is given in Fig. 2 and shows the fact that each of the four physical lines from the vessel are separately represented, as are the 16 safety relief valves (v13 to v28) attached to the individual steam lines. In the RETRAN-3D model, the four lines are

combined into a single line following the header (control volume 980), with the steam flowing to either the turbine inlet (990), or to the condenser (995) via the bypass valves (v29).

Since, for a turbine trip event in KKL, the plant control and protection system plays a major role in the response of the system, the RETRAN-3D representation required substantial improvements compared to that used in [1]. These improvements were, in part, necessary due to plant modifications to the turbine, including the bypass valves.

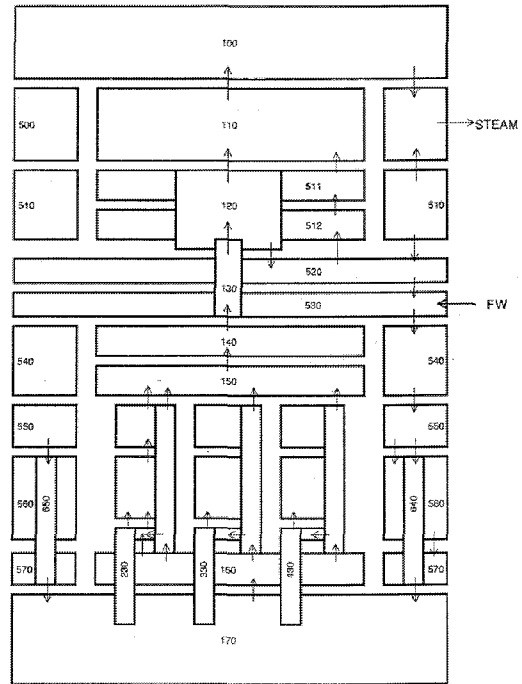


**Fig. 1: RETRAN-3D Vessel Nodalization**

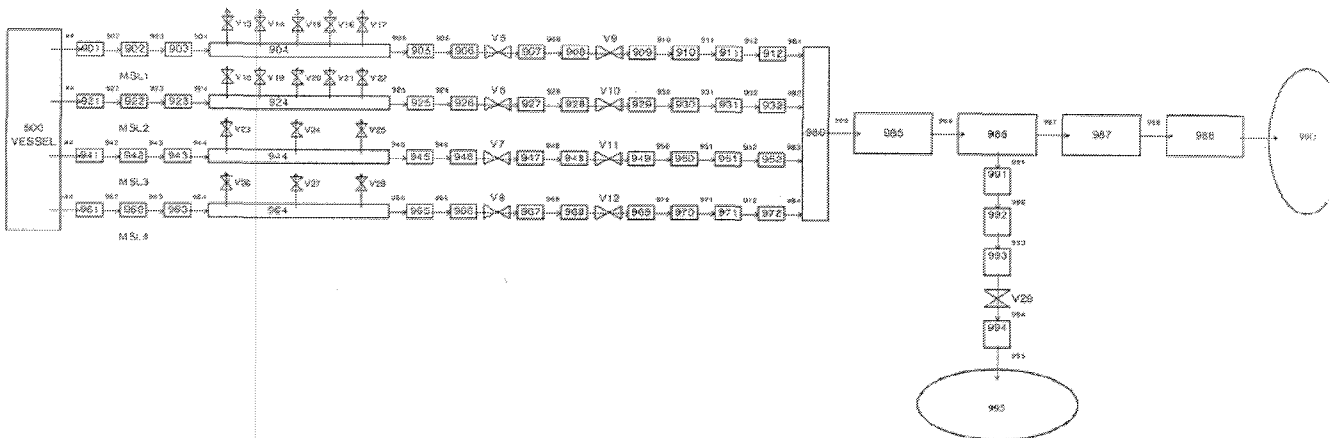


**Fig. 2: RETRAN-3D Steam Line Nodalisation.**

In particular, these included a revision of the pressure regulator transfer function, the addition of the special bypass valve opening logic, and a revision of the control system limits for operation up to 115% power.

In addition to upgrades to the control logic, the RETRAN-3D model was further refined to improve the steam and bypass line pressure drops using the manufacturer's data, to characterize the RETRAN-3D recirculation line flow control valves (FCV) to obtain the correct core flow as a function of FCV position, and finally to provide a transfer function to characterize the turbine bypass steam flowrate as a function of the flow area of a RETRAN-3D "valve", again making use of the manufacturer's data.

The RETRAN-3D 1-D neutron cross-sections were prepared from a CASMO-SIMULATE core-follow calculation using the radial collapsing code SLICK [2]. Since the first calculations of the turbine trip test were pre-test calculations, the core-follow calculations were performed up to the anticipated time of the test using the projected control rod patterns, including that for the test itself.

## 4 PRE-TEST CALCULATIONS

### 4.1 Comparison with Plant Data

The RETRAN-3D calculations performed prior to the test (i.e. blind calculations) are presented in this section, together with a comparison against the measured plant data.

The turbine trip test in KKL was initiated by the closure of the turbine stop and control valves, and the rapid opening of the bypass valves; comparison of the measured and calculated control and bypass valve position during the first second is shown in Fig. 3. (Note that although, for a turbine trip event, the closure of the TSVs primarily controls the flow of steam to the turbines, in this Figure only the plant data control valve position, and not the stop valve position, is shown.) Also shown in Fig. 3 are two RETRAN-3D bypass valve curves. These two curves represent the positions of the bypass valve with and without a 70ms pause in the opening. (The 70ms pause was introduced to simulate the opening pause observed in this and previous turbine trip tests.)

In Fig. 4 we show the bypass valve position during the first 20 seconds, at the end of which time the transient is close to a new steady-state condition. The short-term response (0 to 5 seconds) of the turbine inlet and steam dome pressures is shown in Fig. 5, and the resultant steam flow in Fig. 6. In Fig. 7, we show the reduction in the core inlet flow, while a comparison of the equivalent recirculation line valve area is given in Fig. 8. (Note that the equivalent RETRAN-3D valve area,  $A$ , is related to the physical valve position,  $x$ , through the expression:  $A = 0.1 + 0.1x + 0.8x^2$ .) The measured and calculated core inlet flow is taken from the sum of the flows through the jet pumps. Finally, the core power is shown in Fig. 9.

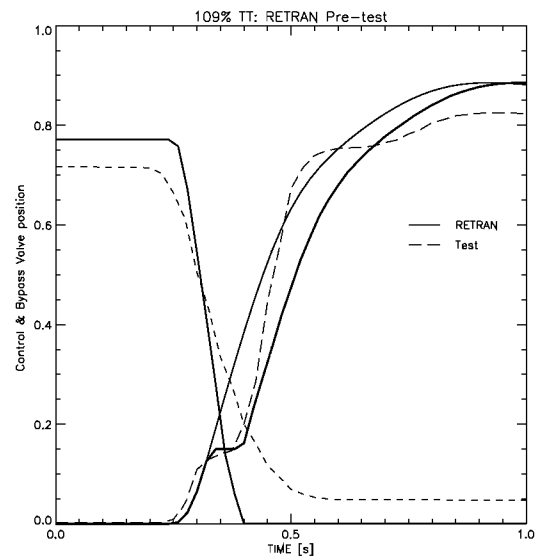


Fig. 3: Control and Stop Valve Position 0 to 1.0 s.

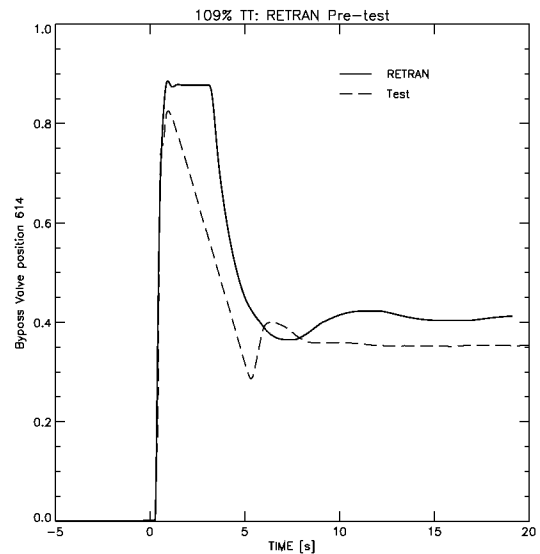


Fig. 4: Bypass Valve Position, 0 to 20 s.

Before commenting on the comparison shown in the above Figures, it is necessary to compare the steady-state conditions just prior to the test against the test boundary conditions. These are presented below in Table 1. Three columns are given in this Table: first, the specifications for the test; second, the initial conditions of the RETRAN-3D pre-test calculations; and third, the conditions used for the initiation of the test. The differences between the test specifications and the RETRAN-3D calculations are very small, while there are just two discrepancies of significance between the pre-test specifications and the actual plant state and test boundary conditions.

Firstly, the core flow was set at 87.5% and not at 91.5%, as in the pre-test specification, and secondly, the control rod banks used for the SRI were changed from banks 39 and 43 to banks 39 and 40. Since bank 40 is closer to the centre of the core, and contains rods which are not fully withdrawn, this change will (and does) produce a greater reactivity insertion, and therefore a larger short-term and long-term power reduction.

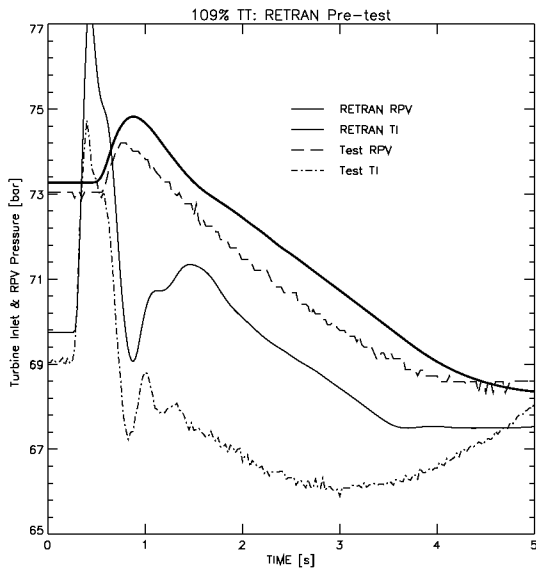


Fig. 5: Turbine Inlet and RPV Pressure.

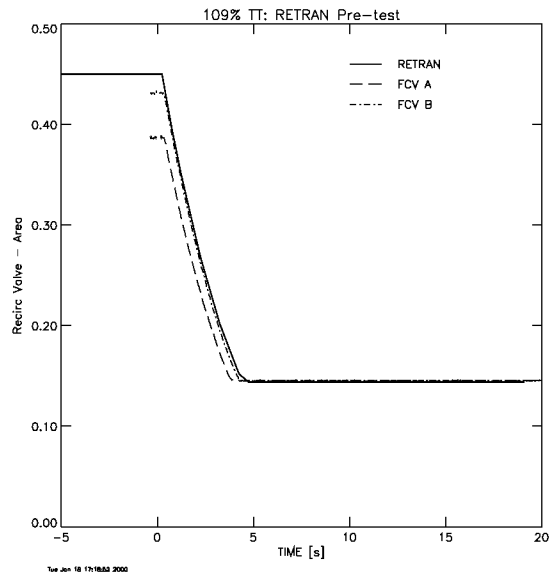


Fig. 8: Recirculation Loop Valve Position.

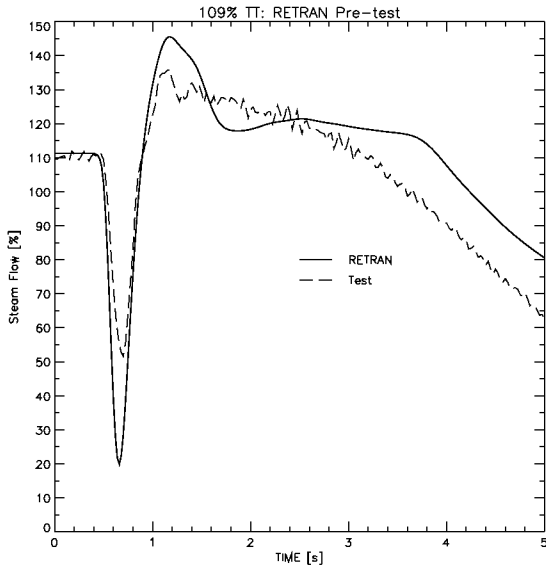


Fig. 6: Steam-Line Mass Flowrate, 0 to 5s.

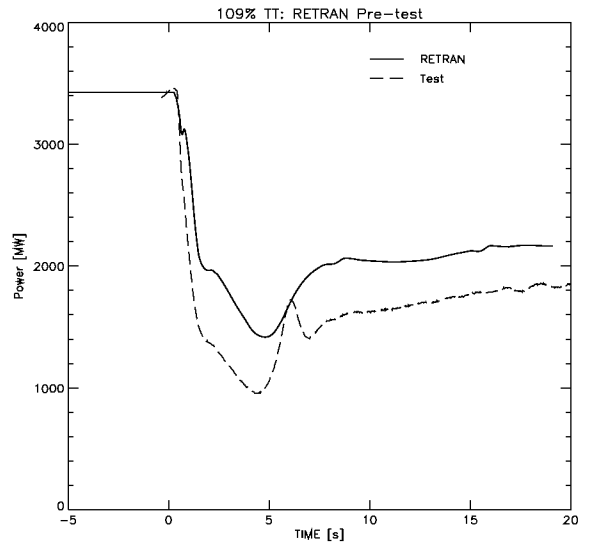


Fig. 9: Core Power.

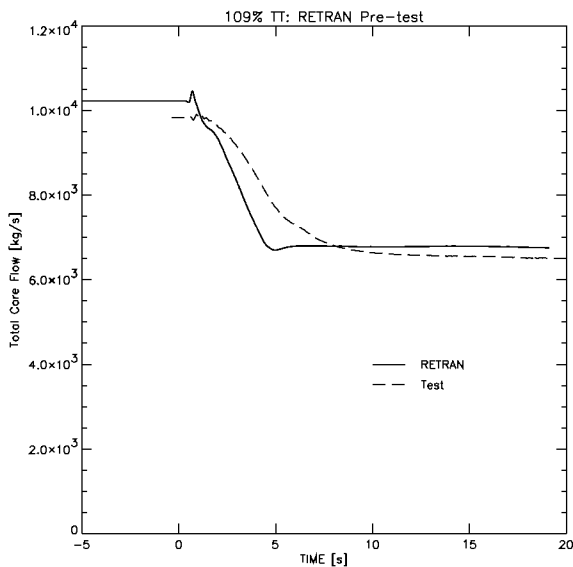


Fig. 7: Total Core Inlet Flow.

This consideration should therefore be borne in mind when reviewing the comparison between the pre-test calculations and the plant data presented above, since the change in SRI rod banks influences both the short-term and long-term power (Fig. 9), the long-term steam flow, and consequently the steam-line pressure drop and final bypass valve position (Fig. 4), etc. Given this limitation, the “general shape” of the core power pre-test calculation is in good agreement with the test data.

The reduction in the core flow (Fig. 7) as a consequence of the closure of the FCVs is in good agreement with the measured data, once again keeping in mind the change in the initial core flowrate from 91.5% to 87.5%, and therefore with the different initial FCV positions. The calculated reduction in the recirculation line and core mass flowrates shows consistently a more rapid response than that observed in the plant data, and it is generally agreed that this comes

from the long time-constant for these measurements, which was not included in the pre-test calculations.

The short-term, ie 0 to 10s, response of the turbine inlet and RPV pressure, and the steam flow along the steam lines, is controlled initially (i.e. within the first second) by the relative closure of the turbine stop and control valves, the opening of the bypass valves, and later by the response of the plant control system to the system behaviour and, in particular, to the turbine inlet pressure. Therefore, in order to understand the nature of the RETRAN-3D pre-test calculations, and their comparison with the plant data, it is necessary to review the representation of the plant pressure control system within the RETRAN-3D model for KKL.

**Table 1:** Test Initial Conditions.

|                                   | Test Specif <sup>n</sup> . | RETRAN-3D | Plant Data |
|-----------------------------------|----------------------------|-----------|------------|
| Core Power (MWt)                  | 3420                       | 3426      | 3425       |
| Steam Dome Pressure (bar abs.)    | 73.1                       | 73.28     | 72.2       |
| Turbine Inlet Pressure (bar abs.) | 69.7                       | 69.8      | 68.35      |
| Total Steam Flow (kg/s)           | 1887                       | 1891      | 1886       |
| Core Flow (kg/s)                  | 10202                      | 10205     | 9746       |
| Core Flow (%)                     | 91.5                       | 91.5      | 87.4       |
| Recirc. Drive Flow (kg/s)         |                            | 1649      | 1589, 1599 |
| FCV position A/B                  |                            | 0.6       | 0.5/0.54   |
| Narrow Rng Level (cm)             |                            | 91        | 94.7       |
| SRI Rod Banks                     | 39 & 43                    | 39 & 43   | 39 & 40    |

#### 4.2 RETRAN-3D Representation of the Plant Control Logic

The plant control system used within RETRAN-3D was developed from that obtained as part of the original input model for KKL [1]. The conversion of the original TRAC input to a form to be used with the RETRAN-3D code is described in [2]. As part of the procedure of benchmarking, the RETRAN-3D model description of KKL [3], and the pre- and post-test calculations of the turbine trip test from 109% power described here, significant revisions were made to the RETRAN-3D representation of the pressure controller part of the control system.

The RETRAN-3D representation of the pressure controller can be described by the block diagram shown in Fig. 10, which shows those elements of the control system flow diagram which relate to the opening and subsequent control of the turbine bypass valves.

Diagrams showing the complete control system logic contained in the original input model can be found in [2]. The main elements of the control logic are: the "live steam pressure" just upstream of the turbine

inlets is sensed and subtracted from a reference value; the resultant pressure difference signal is then passed through a "transfer function" logic; this signal is then converted into a percentage steam flow (block 3) in which a pressure difference of 2.0704 bar corresponds to a steam flow of 100%; the pressure controller signal (percentage steam flow) flow path to the turbine bypass valves first passes through a function which converts the percentage steam flow into a turbine bypass demand signal and, as part of the upgrade of the control logic, a revised transfer function was derived using the valve manufacturer's data for the steam flow versus bypass valve position. Using this information, the percentage steam flow signal could be directly related to a valve position. Secondly, in the revised representation of the bypass valve control system, an additional logic step was added to control the initial opening rate of the bypass valves.

Finally, a transfer function was used to convert the plant valve position signal to a RETRAN-3D valve flow area. This transfer function was developed using the following procedure, to preserve the same steam mass flowrate through the plant and the RETRAN-3D valve. The total bypass valve flow area in the RETRAN-3D model was determined from previous analyses, and a simple stand-alone RETRAN-3D model was then constructed to determine the steam mass flowrate through this valve as a function of the valve relative flow area. The pressure at the valve throat in the stand-alone model was adjusted to be the same as that used to determine the plant valve characteristics. In the RETRAN-3D model, the flow through the valve is governed by critical flow, so that the flowrate is a simple linear function of the valve area.

In addition to the representation of the plant control logic, the RETRAN-3D model included a logic block to simulate the "mechanical" pause in the opening of the bypass valves, as shown in Fig. 3, for example.

#### 4.3 Bypass Valve Demand Signal and Position

In order to gauge the adequacy of the revised model, the calculated bypass valve demand signal from Blocks A and B in the logic diagram (Fig. 10), together with the resultant valve position from Block C, are compared in Fig. 11 with the measured signals from the turbine trip test. (It should be noted that the calculated valve position, Block C in Fig. 10, is upstream of the transfer function, which converts the valve position into an equivalent RETRAN-3D valve area.) A number of observations can be made.

- Firstly, the initial timings are somewhat arbitrary, since the calculated valve position includes the 70ms pause which is part of the valve opening mechanism in the plant.
- Secondly, the bypass position rises to that of the demand signal, and remains at that value, together with the demand signal, until after 3 seconds. The shoulder in the demand signal occurs at about 67% in the RETRAN model, and at 76% in the plant data.

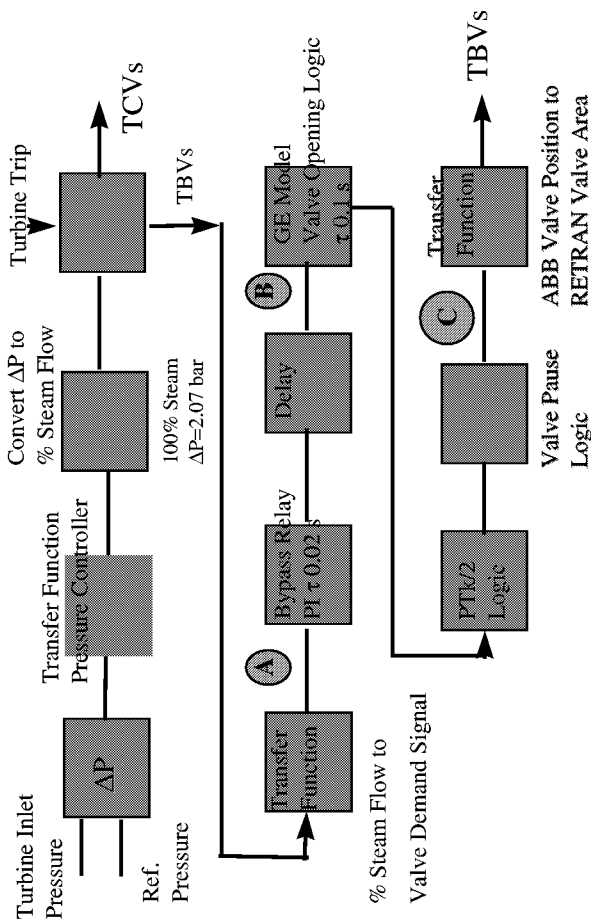


**Fig. 10:** RETRAN-3D Representation of the Bypass Control Logic.

The calculated value comes from a transfer function deduced from the valve bypass data such that the initial 109% steam flow of 1885 kg/s corresponds to a bypass valve position of 67%.

- Thirdly, following the shoulder, the measured and calculated increase in the bypass demand signal comes from the rapid rise in the turbine inlet pressure (Fig. 3) as the turbine stop valve closes. The rate of increase in the calculated and measured demand signal is then dependent on the magnitude of the turbine inlet pressure and the transfer function, and we see that this is faster in the calculation than in the measured plant data.
- Fourthly, the limit in the calculated bypass demand signal comes from the limit placed on the maximum percentage steam flowrate signal. In the original control system model, the maximum steam flow was set in Block A (Fig. 10) to be 115.5%, and this was scaled in this analysis for the power updated conditions to 127%. This translates into a valve demand signal of approximately 90%, using the bypass valve data. In the plant measurement, the demand signal increases to close to 100%, before beginning to fall.

The calculated valve position (Block C, Fig. 10), and the measured valve position, also exhibit slightly different behaviour. The initial opening of the measured

plant bypass valve position follows very closely the behaviour of the demand signal, with almost equal rates of increase (apart from the initial pause), while the rate of opening according to the calculation is reduced by an amount equivalent to an additional time constant of approximately 0.1 s.

Finally, following the initial jump in the valve position (to follow the demand signal), the rate of increase in both the measured and calculated bypass valve position (between 0.5 and 1.0s) decreases. However, whereas the plant data shows that the valve begins to close after 1.0s (in line with the fall in the demand signal), the calculated valve position rises to that of the demand signal, and remains at that value, together with the bypass valve demand signal, until after 3 seconds.

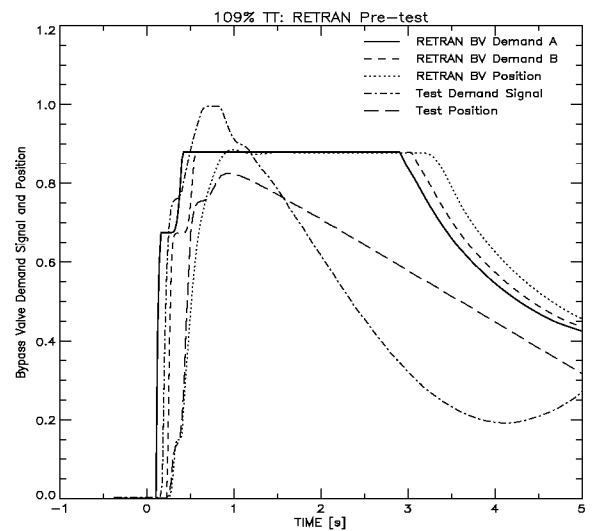


**Fig. 11:** Bypass Valve Demand Signals and Valve Position.

#### 4.4 Turbine Inlet and RPV Pressure

As stated above, the opening and closing of the bypass valves uses the same pressure control logic as that for the turbine valves, and so is determined by the sensed pressure at the entrance to the turbine. The comparison between the calculated and measured turbine inlet pressures is given in Fig. 5. As can be seen from this Figure, after the initial increase in the pressure as the turbine control/stop valves close, and the subsequent fall in pressure as the bypass valves open at approximately 1.0s, the calculated pressure is significantly higher than the measured value. For example, at 1.5s, the calculated pressure is 71.36 bar compared with the measured pressure of 67.42 bar. More importantly, the calculated pressure remains above the steady-state value of 69.7 bar until after 2 seconds. The significance of this is that this pressure equates to a bypass valve demand signal equivalent to a steam flow of 109%. In addition, although the turbine inlet pressure falls below this value at 2.0s, the demand signal does not fall from its limit value until close to 3.0s. One factor which contributes to this delay is the fact that no limits were placed on the first PI controller in Fig. 10. This means that, internal to the

control system, the valve demand is unlimited. The limits placed on the demand signal were imposed further along the signal path.

In spite of the above, the most significant difference between the measured and calculated pressures (after the first second) is in the pressure drop along the steam line. For the steady-state condition prior to the test, the calculated pressure drop is 3.6 bar, compared with the measured value of 3.9 bar. However, after the first 1.5s, whereas the measured pressure drop increases in line with the increase in the steam flow (Fig. 6), the calculated value decreases. The reason for this difference comes from the re-routing of the steam to the bypass valves (Fig. 2).

During the development of the RETRAN-3D input model, use was made of steam-line pressure drop data at 100% power, and at 65% power, to recalculate the overall pressure loss coefficients. In addition, information from the plant defined the pressure drop along the turbine bypass lines for a steam flow of 2182 kg/s, and this then set the overall pressure loss coefficients along these lines. Unfortunately, in the use of the overall steam-line pressure drop data to set the flow resistances, it is not possible to determine the distribution of these losses without additional information. The procedure used therefore, without that information, was simply to scale the losses in the existing input, which included significant losses downstream of the main steam line to bypass line junction. These losses are clearly not included in the flow path if the steam flow is diverted along the turbine bypass flow path, and this explains the reduction in the calculated steam-line pressure drop after the first 1.5s even though the steam flow at this time is in excess of 120%. In addition, the pressure distribution at the junction connecting the bypass line to the main steam line is not correctly accounted for in this model. In particular, the RETRAN-3D pressure change along the steam line when the major part of the flow is directed along the bypass lines has been shown to be in error [4].

The measured data, on the other hand, shows a pressure drop of 4.6 bar at 2 seconds, when the steam flow is ~125 %, which is equivalent to a (steady-state) pressure drop of 3.5 bar for a steam flow of 109%, indicating that almost all of the measured pressure drop is up-stream of the steam-line to bypass-line junction.

Finally, in the plant, there is, during the first 5 seconds, a small residual flow along the steam lines to the feedwater re-heaters, since the valves in these lines take about 5 seconds to close. This flow was not represented in the pre-test RETRAN-3D model.

After the first 1 to 2 seconds, the transient steam flow, both in the calculation and the measured plant data (Fig. 6), is totally consistent with the expected steam flow through the bypass valves. This means that the steam flow can be directly related to the bypass valve position (Figs. 3 and 4) through the bypass valve characteristics.

In summary, after the initial bypass valve opening, i.e. after the first one second, the bypass valve position, and therefore the steam flow etc., is determined by the turbine inlet pressure; this is too high in the pre-test calculation, primarily because of the error in the distribution of the main steam-line flow resistances. One further difference, which is observed in Fig. 4, between the calculated and measured bypass valve position is that during the valve closure the valve closure rate is significantly greater in the calculation than that measured. This difference comes from the fact that, in the plant, the valve closure is limited by the valve characteristics, and this is not included in the RETRAN model. To confirm this, we can see (Fig. 11) that the calculated and plant bypass valve demand signals fall at approximately the same rate, and that the measured valve position falls at a much slower rate than that of the measured bypass valve demand signal.

#### 4.5 RPV Pressure and Steam Flow

Following the initiation of the turbine trip, and closure of the turbine stop valves, the steam flow to the turbine is reduced, and the turbine inlet pressure increases. The increase in pressure therefore propagates back along the steam line as a pressure wave, so that the measured parameters of steam flow and RPV pressure occur some time later. (Note that the measured steam-line flow, Fig. 6, corresponds to a physical location just downstream of the connection to the vessel: i.e., control volumes 902, etc. in Fig. 2.) From Figs. 5 and 6, we see that the steam mass rate begins to decrease approximately 200 to 250ms after the initial rise in the turbine inlet pressure, while the RPV pressure begins to increase after a further 70 to 80ms delay. The delays calculated with RETRAN-3D are approximately 40ms less than the measured values.

The reduction in the steam mass flowrate as the turbine stop valves close, and the bypass valves open, is more pronounced in the calculation than in the plant measurement. However, it should be noted that the instrumentation has a time resolution of ~50ms, which is long on the time-scale of the flow reduction, and this was not included in the pre-test calculation.

After the first half second, the bypass valves are more than 50% open (Fig. 3), and so the "steady-state" flowrate through these valves is more than 1400 kg/s. This sudden increase in the steam flow at the turbine bypass propagates as a rarefaction wave back, first along the bypass line, producing a rapid decrease in the turbine inlet pressure, and then along the main steam line, producing the observed increase in the main steam line mass flowrate beginning at approximately 0.7s (Fig. 6). The rate of the steam mass flowrate increase will be influenced not only by the steam flow into the turbine bypass (and therefore by the bypass valve position), but also the sonic propagation of this information back along the steam line. Because the location of the steam flowrate measurement is so far removed from the bypass valves, i.e. at a distance corresponding to a sonic

a distance corresponding to a sonic propagation time of typically 200ms, it is not possible during this first phase of the transient to directly relate the steam flow through the bypass valves to the measured value. The peak steam flowrate is reached after 1.1 to 1.2 seconds, and the calculated value shows a transient overshoot before it reaches a “steady-state” value after about 1.5 to 2s. This overshoot is not seen so clearly in the measured data, which is partly explained by the 50ms instrumentation time resolution. As was observed above after about 2s, “steady-state” conditions are obtained in both the measured and calculated steam flowrates, i.e. the flowrate is a constant value along the steam line.

#### 4.6 Summary of Pre-Test Calculations and Errors

In the above Sections, we compared the results of the pre-test calculation with the measured plant data and, from this, identified several differences, input model errors and deficiencies. These are summarized below, and were subsequently used as the basis of a post-test and sensitivity analysis of this test.

**Input and Boundary Conditions:** In Section 3.2 above, it was noted that the control rod banks used in the 109% power test were changed from those given in the test specification. This change produced a significant increase in the rod worth of the inserted banks, and so resulted in a greater than calculated power reduction. In addition to the change in the control rod banks, the other obvious difference in the initial and boundary conditions was the change in the core flowrate from 91.5% to 87.5%.

**Steam Line Characteristics:** In Section 3.6, it was clearly seen, from a comparison of the calculated and measured steam-line pressure drop before and during the transient, that there was a significant “error” in the distribution of the pressure loss along the steam line. In order to demonstrate how this distribution influences the results of the calculations, a post-test calculation was performed with a redistribution of the pressure losses along the steam line.

**Turbine Stop Valve Closure and Steam Flow:** Since the initial rise in the turbine inlet pressure is dependant on the reduction in the steam flow into the turbine, and therefore on the rate of closure of the turbine stop valve, a comparison of the stop valve position with the equivalent calculated parameter was made. This showed similar behaviour, except for the final 10%. However, equally important in calculating the residual flow along the steam lines to the turbine is the flow to the feedwater re-heaters, which goes to zero over a relatively long period (typically 5s). A simple representation of this residual flow was included in the post-test analysis.

**Control System Representation:** Several “errors” were identified in the representation of the pressure controller and, in particular, in those aspects which influence the bypass valve opening. Firstly, the bypass demand signal includes an additional time-constant of ~0.1s, and this was removed. Secondly, limits were placed on the first PI integral in the pres-

sure controller, and thirdly, the influence of the 50ms time resolution of the flow instrument on the calculated steam flow was investigated.

**Bypass Valve Closure:** It was mentioned above that the closure of the bypass valves is controlled by the mechanical characteristics of the valves, and not by the control system and the value of the bypass valve demand signal. Since this feature is difficult to include in a computer model, a sensitivity analysis was included to examine the consequences of these characteristics.

## 5 POST-TEST ANALYSIS

In line with the above comments, a series of post-test calculations was performed. Each of these calculations added, in a cumulative manner, one or more model corrections to overcome the above deficiencies. Some results of the individual calculations are presented in the following sections. These concentrate primarily on those parameters modified by the model changes associated with that specific calculation. Finally, a more general review of the final calculation is presented. The post-test analysis was not intended to be a definitive and final analysis, but was performed to examine the model and calculational deficiencies highlighted during the review of the comparison of the pre-test calculations with the measured plant data. However, it is clear that there remain some small differences between the calculations and the measured data.

### 5.1 Run 1: Initial and Boundary Conditions

The first set of post-test calculations were performed to correct for differences between the pre-test initial and boundary conditions; that is, the insertion of rod banks 39 and 40 instead of 39 and 43, and the change in the initial core flow from 91.5% to 87.5%. In addition to these changes, the timing for the insertion of the SRI control rods was revised. The results of these changes can be seen most directly in Figs. 12 and 13, which show the core power and the total core flow, respectively. Included in Fig. 13 is a curve showing the effect of including a 2.5s time-constant to the calculated core flow. As can be seen, this results in a very close agreement between the calculation and the measurement.

The comparison between the revised core power (Fig. 12) and that from the pre-test calculation (Fig. 9) shows a significant improvement in the prediction of both the short-term (1 to 2s) and the long-term (>10s) power. In particular, in the long term, as the reactor re-establishes a new steady-state condition, the calculated and measured powers approach the same value.

This confirms the fact that the “steady-state” power reduction, as a consequence of the control rod insertion and flow reduction, have been correctly calculated. There is, however, still a difference in the transient power reduction as the SRI control rods are inserted.

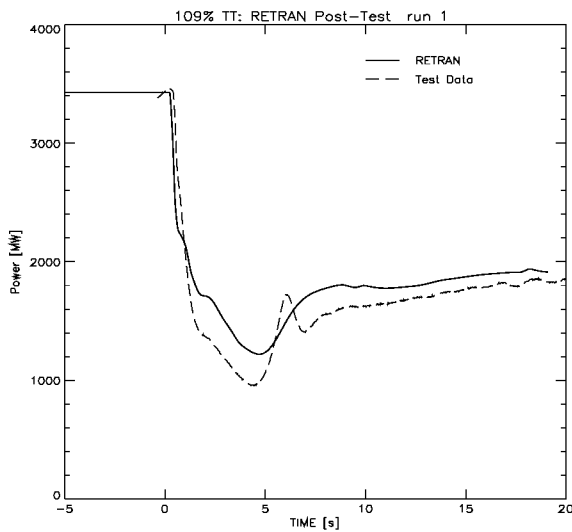


Fig. 12: Post-Test Run 1: Core Power.

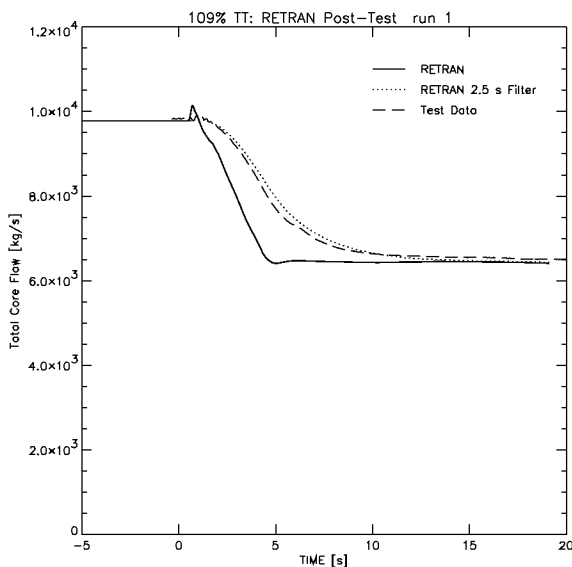


Fig. 13: Post-Test Run 1: Core Flow.

This difference is thought to be associated with the changing 3D flux distribution, and is therefore not captured with the current 1D neutron diffusion calculation. In addition to the possible change in the 3D flux distribution, the 1D representation of the core means that the wide range of steady-state fuel temperature distributions and rod thermal time-constants, which occur as a consequence of the different fuel/clad gap conductivities, are represented by a single equivalent value. The different initial fuel temperatures and rod time-constants will influence the initial power drop by modifying the change in the reactivity feedbacks, through the change in the fuel temperature (Doppler coefficient) and rod surface heat flux (void coefficient).

## 5.2 Run 2: Steam Line Characteristics

As was described above, it was observed during the review of the pre-test calculation that, although the steady-state, steam-line pressure drop is correctly predicted, the calculated pressure drop following the opening of the bypass valve is only about half the measured value. Several features of the plant contrib-

ute to this difference, one the most important of which is the distribution of the steam-line pressure losses, since any pressure loss located between the steam-line to bypass junction and the turbine inlet will not be included in the steam-line pressure drop following the opening of the bypass valves. In addition, the pressure changes at the bypass line to main-steam-line junction as the flow is diverted, and will influence this behaviour.

In order to demonstrate the importance of this effect, the equivalent of two velocity heads was moved from downstream to upstream of the bypass-to-main-steam-line junction. It should be noted that this value was chosen to demonstrate the importance of the distribution of the pressure losses, and is not meant to be a final value.

The results of this calculation can be seen in Figs. 14 and 15, which show, respectively, the measured and calculated reactor pressures (Fig. 14) and the bypass valve demand signal and position (Fig. 15).

The differences between these results and those of the pre-test calculation (Figs. 5 and 11) can be explained as follows: since the steam flow through the bypass valves is choked, the mass flowrate is only weakly dependent upon the upstream pressure, while the strongest dependence comes from the valve position (and therefore the control system), which is "fully" open during the first 2 to 3 seconds. In addition, the pressure in the RPV changes slowly and is determined by the reduction in power, and is again only weakly dependent upon the steam flowrate.

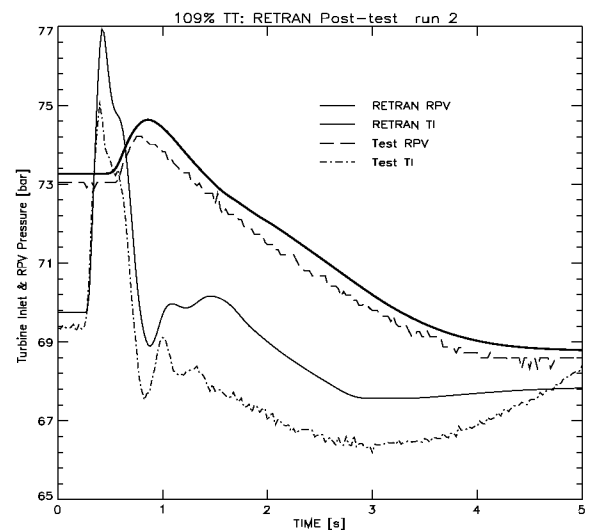
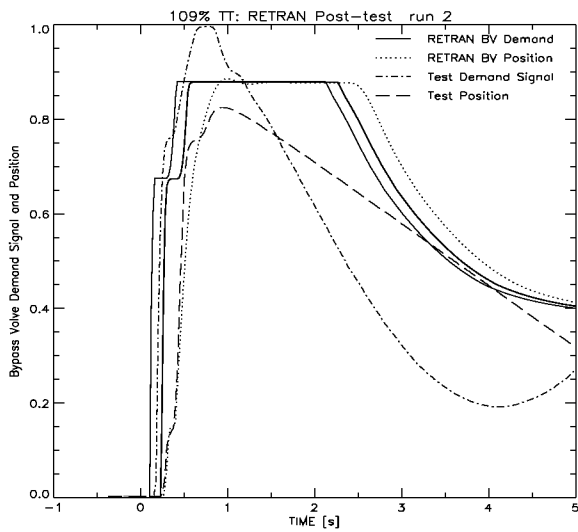


Fig. 14: Post-Test Run 2, Turbine Inlet and RPV Pressure.

Therefore, since the steam mass flowrate and the RPV pressure are relatively independent of the system behaviour during the first few seconds, the parameter which changes as a consequence of the change in the steam-line flow resistance is the turbine inlet pressure, and this can clearly be seen from the comparison of post-test and pre-test calculations shown in Figs. 14 and 5.



**Fig. 15:** Post-Test Run 2, Bypass Valve Demand Signal and Position.

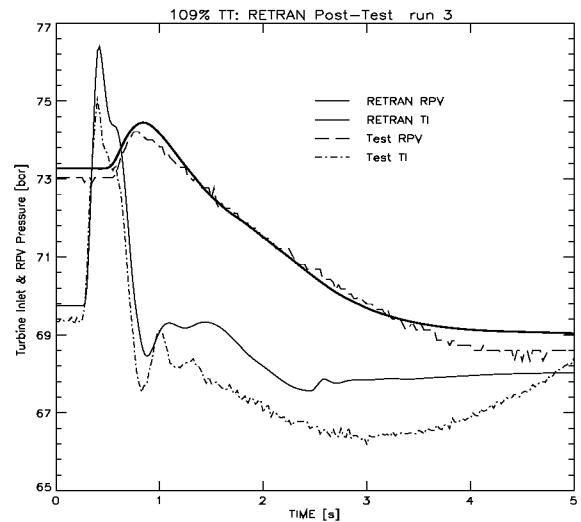
The effect of the reduction in the calculated turbine inlet pressure on the bypass valve demand signal and position can be seen by comparing Figs. 15 and 11. Here we see that the reduction in the turbine inlet pressure (which is the sensed signal for the pressure controller) shortens the time for which the calculated bypass valve demand signal is at its maximum from 3 to 2 seconds

### 5.3 Run 3: Re-Heater Flow

An additional feature of the plant, which was not included in pre-test calculations, was the steam flow to the feedwater re-heaters and other auxiliary equipment. For the post-test calculation, the data for the steam flow to the re-heaters and auxiliary equipment was taken from the plant data acquisition system. This flow decreases to zero over 5 seconds as the re-heater-line valves close. In order to simulate this within the RETRAN-3D model, the re-heater flowrate was translated into a residual flow through the turbine stop and control valves. Again, no attempt was made to “optimize” the input stop/control valve position, since the post-test calculations were performed only to identify and highlight the importance of the various phenomena and features of the plant. The comparisons of the resultant RPV and turbine inlet pressures against the measured data are shown in Fig. 16. It can be seen from a comparison of Figs. 16, 14 and 5 that both the redistribution of the steam-line pressure losses and the re-heater flow considerably improve the prediction of the turbine inlet pressure. The reason for the improvement when the re-heater flow is included comes from the fact that this additional flow increases the steam-line flowrate and, as explained above, since the RPV pressure is relatively independent of the steam flowrate, the turbine inlet pressure must then fall.

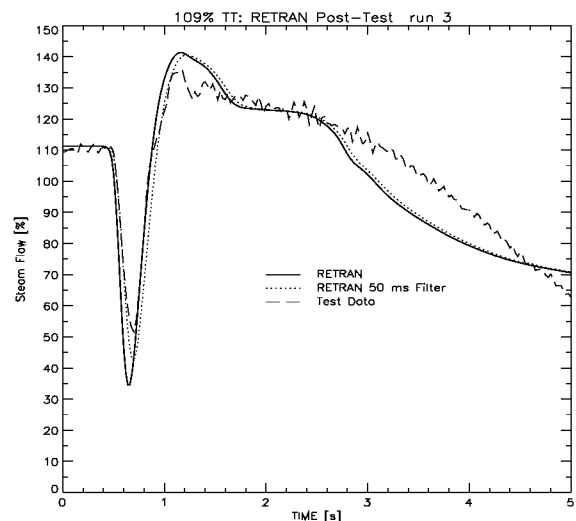
In addition to the above improvements in the RETRAN-3D calculation, the inclusion of the re-heater flow has two further effects. Firstly, the reduction in the steam flow as the turbine stop and control valves close is not as abrupt. The effect of this is shown in

Fig. 17, which gives the steam-line mass flowrate for this calculation. A comparison of this Figure with the equivalent pre-test calculation (Fig. 6) shows a significant improvement in the prediction of the minimum steam mass flowrate. Also included in Fig. 17 is a curve showing the steam flowrate after passing through a 50ms filter, as calculated by RETRAN, making it therefore more directly equivalent to the measured flowrate.



**Fig. 16:** Post-Test Run 3, Turbine Inlet and RPV Pressure.

Secondly, as a consequence of the less abrupt reduction in the steam-line flow during the turbine stop and control valve closure, the peak in the turbine inlet pressure is reduced. The calculated pressure increase is now 6.7 bar compared with a pre-test value of ~7.7 bar, and a measured value of 5.8 bar. This can be seen more clearly in Fig. 18, which gives a comparison of the change in the pre- and post-test turbine inlet pressure.



**Fig. 17:** Post-Test Run 3, Steam-Line Mass Flowrate.

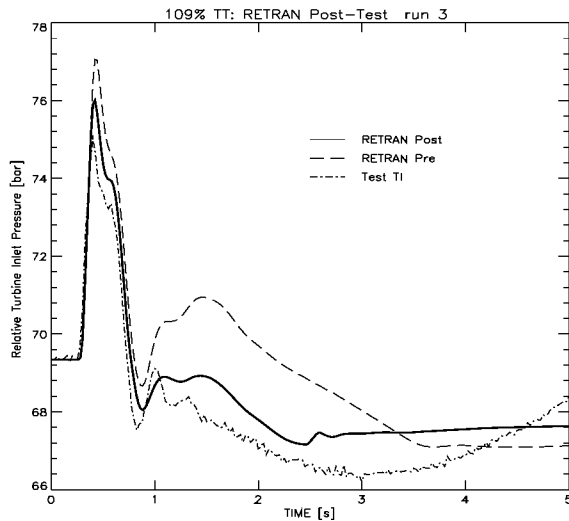


**Fig. 18:** Change in Turbine Inlet Pressure.

Finally, the reduction in the initial increase in the calculated turbine inlet pressure produces a corresponding reduction in the rise in the RPV pressure, which is now smaller than the measured value. This difference occurs because of the diffusive nature of the RETRAN numerical scheme.

#### 5.4 Control System Changes and Bypass Valve Closure Rate Limit

Two “errors” in the revised representation of the pressure controller were identified as part of the review of the pre-test calculations. These were the inclusion of an additional time-constant of  $\sim 0.1$ s in the bypass valve demand signal, and the lack of limits on the first PI controller in the pressure controller. In the revised calculation, the 0.1s time-constant was removed, and an upper limit was placed on the PI integral. In order to determine the value of this limit, use was made of the fact that the effect of the “Maximum Combined Flow Limiter was adjusted to initiate at a total steam flow of 2120 kg/s.” A limit was therefore placed on the integral of 124.7% (i.e. the ratio of a steam flowrate limit of 2120 kg/s to the nominal 100% steam flowrate of 1700 kg/s).

The final post-test model change to be included as part of the review of the pre-test analysis was to impose a limit on the bypass valve closure rate. The closure-rate limit was set to 13%/s; this value was simply taken from the observed plant data.

In addition to the model improvements which were produced as a consequence of the comparison of the pre-test calculations with the plant data, a further update was included to reflect the fact that the bypass valve opening logic was modified during the plant outage immediately before the test, and was therefore not included in the pre-test calculations.

The influence of the above changes to the control logic on the calculated bypass valve demand signal and position is shown in Fig. 19, where again the calculated valve position is taken from Block C in Fig. 10; i.e., immediately upstream of the valve position to RETRAN-3D valve area transfer function. In order to

obtain the correct behaviour following the pause in the plant bypass valve opening, the calculated and measured valve positions were matched immediately following this pause at 400ms. This was necessary because the initial pause is caused by the valve mechanics, and not by the control logic. Figure 19 shows a distinct improvement in the calculation of the bypass valve position in that the calculated valve position now mirrors the demand signal in the same manner as in the plant. The under-prediction of the calculated valve position after about 0.5 to 0.6 seconds therefore merely reflects the under-prediction of the bypass valve demand signal.

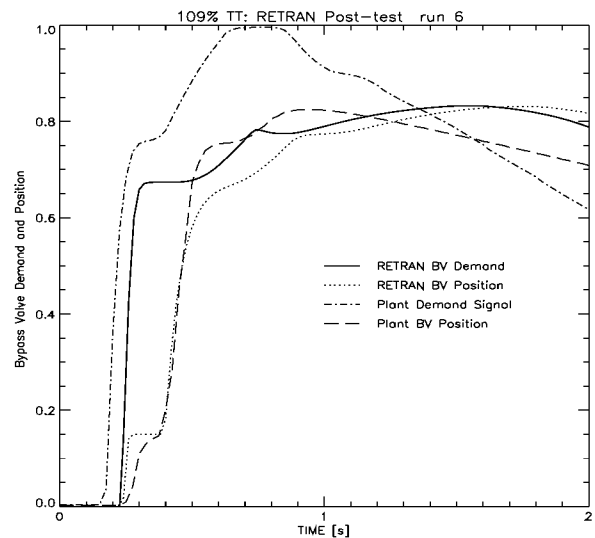


**Fig. 19:** Post-Test Final Bypass Valve Position from 0 to 2s.

The long-term bypass valve position is shown in Fig. 20, and the steam mass flowrate in Fig. 21. As a consequence of the improvement in the bypass valve opening, the maximum steam flowrate (Fig. 21) is now in closer agreement with plant data. In the longer term, i.e. after 1.5 to 2 seconds, when the steam flowrate is approximately constant along the steam line, the calculated steam flowrate is initially lower than the measured value, even though the final valve position (Fig. 20) is greater. This is consistent with the plant observation that the measured steam flowrate through the bypass valves is greater than that given in the manufacturer’s data curves.

#### 5.5 Post-Test Calculation Summary

The results of the post-test calculations presented above, which include the model improvements and changes identified as part of the review of the pre-test calculations, and the upgrade to the bypass valve control logic, show a significant improvement in the quality of the RETRAN-3D calculations. A summary of the “improvement” in the post-test versus the pre-test calculations is shown in Figs. 22 to 25, which show a comparison between the pre-test, post-test and the plant data for the bypass valve position, turbine inlet pressure, steam flowrate, and core power, respectively.

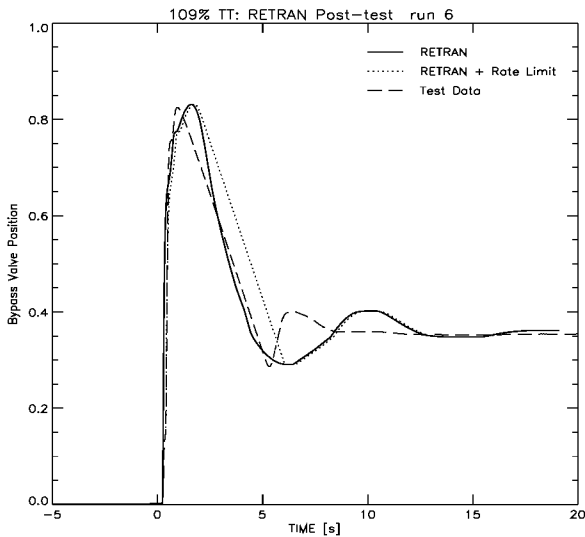


**Fig. 20:** Post-Test Final Bypass Valve Position from 0 to 20s.

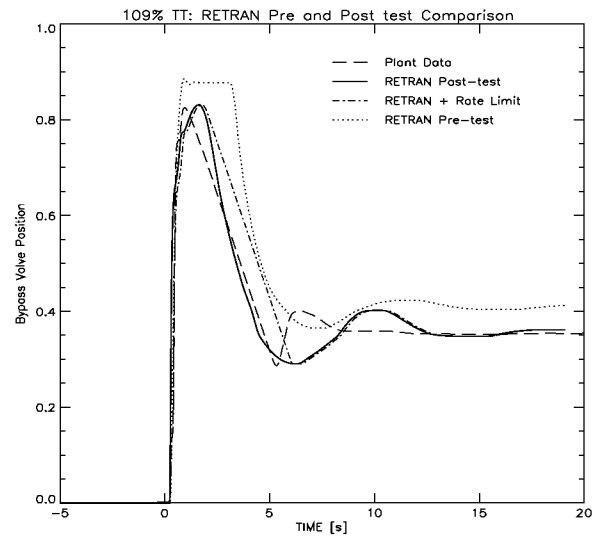


**Fig. 22:** Bypass Valve Position from 0 to 20 s.

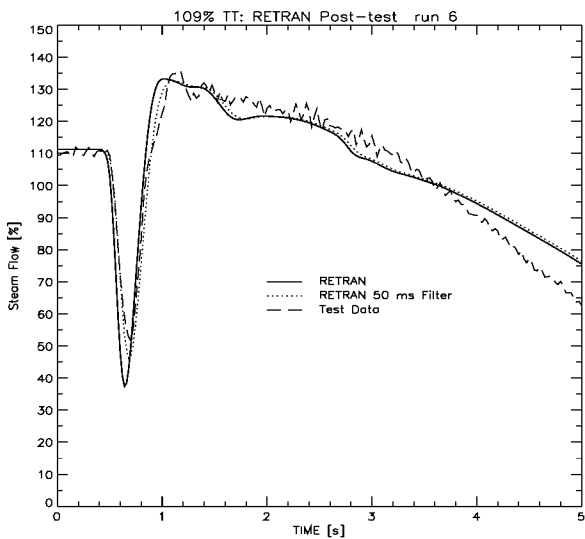


**Fig. 21:** Post-Test Final Steam-Line Flowrate.

During the course of the post-test analysis, two further differences between the calculations and the measured data were identified which warrant further investigation. These are: firstly, the under-prediction of the immediate power reduction as a result of the selected control rod insertion, and secondly, the possible correction of the bypass valve flow characteristics deduced from plant measurements.

## 6 SUMMARY AND CONCLUSIONS

As part of the PSI/HSK STARS project, pre-test calculations were performed using the RETRAN-3D code for the KKL turbine trip at 109% power. In this paper, we present the results of these pre-test calculations, together with a description of the turbine trip test, and a comparison of the results with the measured plant data.

We then discuss in greater detail the differences between the pre-test results and the plant measurements, including the differences in the initial and boundary conditions, and how these differences influence the calculated and measured results.

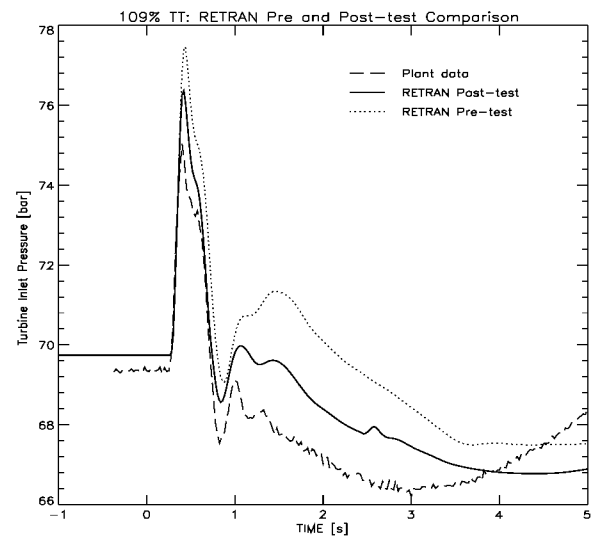


**Fig. 23:** Turbine Inlet Pressure.

The results of the pre-test (i.e. blind) calculations show good overall agreement with the experimental data, particularly for the maximum in the steam-line mass flowrate following the opening of the turbine bypass valves. This is of critical importance, since the steam-line flow has the least margin to the reactor scram limit.

The agreement is especially good since major changes were made during the course of the pre-test analysis to the pressure controller logic obtained as part of the original input model. These changes included the use of the bypass-valve design data to characterize the steam flow through the equivalent "RETRAN" valves. Finally, the comparison was influenced by the fact that the control rod banks used in the test for the SRI were changed from those given in the test specification in order to produce an increased power reduction.

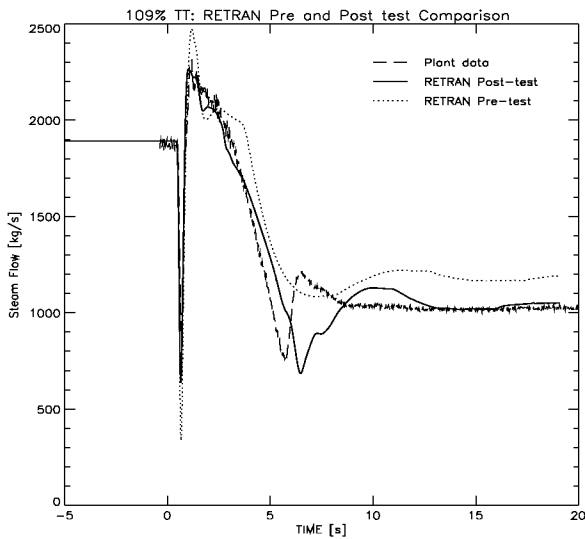


Fig. 24: Steam Line Mass Flowrate.

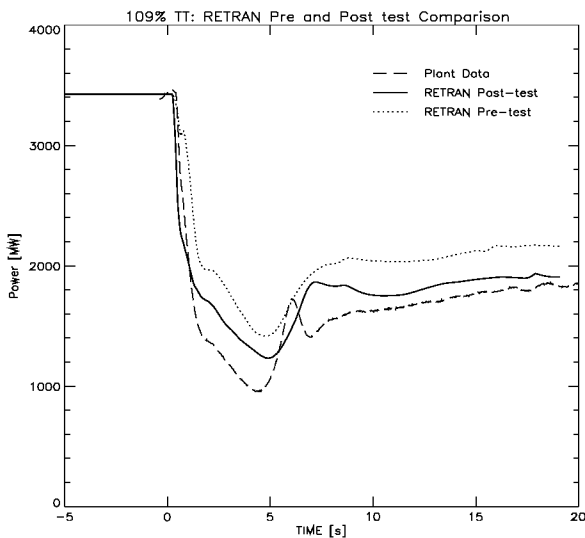


Fig. 25: Core Power.

As a consequence of the comparison of the pre-test calculations against the measured data, several deficiencies in the RETRAN-3D model were identified, and corrected, as part of a post-test analysis. The modifications included the following:

- The correction of the initial and boundary conditions to those used in the test, the most critical of which was the use of the correct control rod banks for the SRI, since this had a significant effect on the short- (~1.0 s) and long-term reactor power.
- The redistribution of the pressure losses along the main steam lines, and the modification of the turbine inlet flow following the trip of the turbine, to include the steam flow into the feedwater re-heaters. These changes significantly improved the prediction of the turbine inlet pressure, and therefore the response of the main pressure controller.

- Some small remaining deficiencies in the RETRAN-3D model of the pressure control logic were identified and corrected. These produced an improved prediction of the bypass valve demand signal, and the resultant bypass valve position.
- The bypass valve opening logic was modified to reflect the changes made to the plant logic during the plant outage immediately prior to the test.

The post-test analysis allowed for both an improvement in the calculated results and a deeper understanding of the behaviour of the turbine trip transient. Finally, during the course of the post-test analysis, two further differences between the calculations and the measured data were identified which warranted further investigation. These are: the under-prediction of the immediate power reduction as a result of the SRI, which will be investigated as part of the implementation of a RETRAN-3D 3-D kinetics model, and a revision of the flow characteristics of the bypass valves from the design data to that measured during the course of plant tests.

## ACKNOWLEDGMENTS

The author would like to acknowledge Dr. J. Klügel (HSK) and Mr H. Eitschberger (KKL) for their many helpful comments. This work was partly funded by the Swiss Federal Nuclear Safety Inspectorate and the Swiss Federal Office of Energy.

## REFERENCES

- [1] P. Coddington and M.A. Zimmermann, "TRAC-BF1 Input Manual for KKL and Conversion from TRACG", TM-41-96-11, PSI Internal Report, 1996.
- [2] P. Coddington, F. Holzgrewe, D. Maier, "Development of a RETRAN-3D Input Model for the Kernkraftwerk Leibstadt Boiling Water Reactor (on Call #10)", TM-41-98-33, PSI Internal Report, 1998.
- [3] P. Coddington, "Analysis of BWR/6 Startup Tests with RETRAN and TRAC", PSI Annual Report, Annex IV, 1997.
- [4] W. Barten, P. Coddington, J. Sullivan, "Development of a Model for RETRAN-3D for Pressure Losses at T-Junctions", paper to be published, ICONE9 Conference, Nice, France, April 2001.